

ARL 64-56

**CHARTS FOR USE WITH HYPERSONIC
AIR WIND TUNNELS**

**WILLIAM G. REINECKE, 1/LT. USAF
HYPERSONIC RESEARCH LABORATORY**

APRIL 1964

Project 7064

**USAF: AEROSPACE RESEARCH LABORATORIES
OFFICE OF AEROSPACE RESEARCH
UNITED STATES AIR FORCE
WRIGHT-PATTERSON AIR FORCE BASE, OHIO**

FOREWORD

This report was prepared by the Hypersonic Research Laboratory of the Aerospace Research Laboratories under Project 7064, entitled "Hypersonic Flow Research."

The author gratefully acknowledges the contributions made to this note by Lt. J. S. Petty and by Messrs. K. S. Nagaraja, Anthony Fiore, and Merle Stratton.

ABSTRACT

This report contains a series of graphs for use with hypersonic, air wind tunnels and is most conveniently used in conjunction with NACA Report 1135, "Equations, Tables, and Charts for Compressible Flows." The data presented differ from those in NACA 1135 in the following ways: data are computed for higher total temperatures, viscosity data due to Bromley and Wilke are used in the low static temperature regime, mean free path data are given, and the variation of γ with temperature is considered in all the computations. The graphs are plotted for any total pressure (within the range of validity of the analysis), for total temperatures through 5000°R, and for Mach numbers through 30. The computed data are also used to determine an empirical relation between the Knudsen, Mach, and Reynolds numbers.

NOTATION

The notation in this report is the same as that of NACA Report 1135, "Equations, Tables, and Charts for Compressible Flows."¹ However, some additional symbols are introduced.

SYMBOLS

A	Cross sectional area of stream tube (inches ²)
a	Speed of sound (ft/ sec)
C _{ij}	Constants (dimensionless)
F	Function of M defined in text (dimensionless)
I, J	Integers (dimensionless)
i, j	Exponents and indices (dimensionless)
Kn	Knudsen number, λ / l (dimensionless)
Ln	Logarithm to the base e
l	Characteristic length (inches)
M	Mach number, V/a (dimensionless)
m	Mass flow rate (slugs/sec \times lbf)
p	Pressure (lbf/ inch ²)
q	Dynamic pressure, $\rho V^2 / 2$ (lbf/ inch ²)
R	Gas constant, 1716 (ft ² / sec ² \times °R)
Re	Reynolds number, $\rho V l / \mu$ (dimensionless)
T	Temperature (°R)
V	Speed (ft/sec)
γ	Ratio of specific heats (dimensionless)
λ	Mean free path (inches)
μ	Viscosity (slugs/ ft \times sec or lbf \times sec/ ft ²)
ρ	Density (slugs/ ft ³)

Contrails

SUPERSCRIPTS AND SUBSCRIPTS

- ()* Conditions where the gas is moving with sonic speed
- ()_t Total or isentropic stagnation conditions
- ()₁ Conditions just upstream of normal shock wave
- ()₂ Conditions just downstream of normal shock wave
- ()_{t1} Total conditions just upstream of normal shock wave
- ()_{t2} Total conditions just downstream of normal shock wave
- ()_{Perf} Quantity evaluated for a gas obeying the perfect gas law
(thermally perfect) and with constant γ (calorically
perfect)
- ()<sub>Therm
Perf</sub> Quantity evaluated for a gas obeying the perfect gas law,
but with γ varying with temperature (thermally perfect
only)

Contrails

INTRODUCTION

Experimentalists using supersonic, air wind tunnels have long relied heavily upon NACA Report 1135, "Equations, Tables, and Charts for Compressible Flow," by the Ames Research Staff¹. However, the development of an ever broadening regime of supersonic wind tunnel tests suggests the usefulness of some additions to the data presented therein. Higher total temperatures are of interest when it is necessary to simulate the static temperatures, densities, and mean free paths characteristic of high altitude hypersonic flight. Moreover, recent data presented by Daum² suggests that hypersonic wind tunnels may also be run liquefaction free at static temperatures lower than previously thought possible. These new conditions in the test section require additional data and charts for use in conjunction with existing ones. The high temperature, low density conditions warrant a more detailed charting of the effects of the variation of gamma with temperature and also suggest a need for a graph of mean free path versus wind tunnel parameters. On the other hand, the possibility of low static temperatures coupled with recent low temperature viscosity determinations³ requires the recalculation of Reynolds number versus tunnel parameters in this range.

This note was prepared to fulfill these needs. The data herein presented were originally intended only for use within the Aerospace Research Laboratories (and, to some extent, the parameter range was dictated by ARL facilities), but the generality of the charts suggested that they be made available in a technical report.

CONSIDERATION OF NONCONSTANT GAMMA

The equations describing the flow of a compressible gas may be integrated immediately under the following assumptions: the flow

Contrails

is one dimensional and steady, the gas is thermally perfect ($p \sim \rho T$), the gas is calorically perfect ($\gamma = \text{constant}$), and the gas is inviscid and nonconducting. This analysis is given in detail in Reference 1. In the present report one of these assumptions is relaxed: γ is allowed to be a function of temperature only; that is, the gas is considered calorically imperfect. The effects of caloric imperfections in the one dimensional flow equations may be accounted for if γ is a known function of temperature. In this case, the solution becomes a function of total temperature as well as Mach number. This analysis is also carried out in Reference 1. All the data presented in the present report were calculated using a form for γ which varied with temperature as given in Reference 1.

Now as the gas is accelerated through a wind tunnel, eventually the static temperature reaches a value below which γ is nearly constant. For lower static temperatures and higher Mach numbers the ratio between the one dimensional flow dependent variables (for example, T/T_t) computed for constant and nonconstant γ remains constant. This may be seen from the algebraic form of the corrections for varying γ given in Reference 1 (for example, equation 186) and is illustrated in Charts 9 through 20 of that reference. Specifically, for total temperatures of 5000°R and less, the correction factors become constant for Mach numbers greater than about seven (depending on the variable of interest and upon the total temperature). Then we may graph these correction factors versus total temperature only for Mach numbers greater than about seven. This has been done in Figure 1, which is simply a cross plot of the asymptotes of the above-mentioned charts of Reference 1.

Figure 2 is a graph of the mass flow through an air tunnel per unit throat area, per unit total pressure versus total temperature.

The function plotted is

$$\frac{m}{p_t A^*} = \frac{p^*}{p_t} \sqrt{\frac{\gamma^*}{RT^*}}$$

and depends only upon total temperature.

CONSIDERATION OF VISCOSITY AT LOW TEMPERATURES

In the test section of a supersonic, air tunnel whose total temperature is 5000°R or less, the Sutherland equation for viscosity,

$$\mu = 2.27 \times 10^{-8} \frac{T^{3/2}}{T + 198.6},$$

will provide an acceptable value for the viscosity, providing the total temperature is not too low. However, when the test conditions are such that the static temperature is less than about 200°R, the Sutherland value for viscosity becomes doubtful. Low temperature viscosity data (somewhat higher than the Sutherland values) due to Bromley and Wilke³ and presented by Gregorek and Lee⁴ (see footnote) may be used at these lower temperatures. For the computations in the present report, 180°R was chosen as the border between the Sutherland law and a parabolic fit to the Bromley and Wilke data. The parabola used was

$$\mu = 10^{-8} (0.887 + 0.0663T + 0.0000589T^2), \quad 0 < T < 180.$$

At the matching point of 180°R, this equation gives a value of viscosity 1.8% higher than the Sutherland equation. Since this figure

Footnote: The vertical axis of the viscosity plot, Figure 19, in Reference 4 is mislabeled. The line labeled "0" should be "2"; the line labeled "2" should be "4", etc.

of 1.8% represents about the reading uncertainty of the viscosity and Reynolds number graphs, no attempt was made to smooth the transition. Figure 3 is a plot of this viscosity function versus temperature.

Finally, Figure 4 is a graph of Reynolds number per unit length, per unit total pressure plotted versus Mach number for various total temperatures. In calculating the data presented in Figure 4, the above described viscosity law was used. The function plotted is

$$\frac{Re}{lp_t} = 12 \frac{p}{p_t} \frac{M}{\mu} \sqrt{\frac{\gamma}{RT}}$$

and depends upon Mach number and total temperature.

CONSIDERATION OF THE MEAN FREE PATH

The mean free path of a gas at rest is usually taken to vary inversely as the density⁵. However, the mean free path depends upon the frame of reference in which it is evaluated. Thus the characteristic mean free path of a wind tunnel test section depends not only on the density in the test section, but also upon the Mach number there. This dependence of the mean free path upon Mach number has been analyzed by Muckenfuss⁶. Using the hard sphere molecular model, he shows that the mean free path in a moving gas is given by

$$\lambda \sim \frac{1}{\rho} F(M),$$

where

$$F(M) = \frac{1}{2} \text{Exp} \left(-\frac{5}{6} M^2 \right) + \sqrt{\frac{\pi}{120}} \left[\frac{5M^2 + 3}{M} \right] \text{Erf} \left[\sqrt{\frac{5}{6}} M \right].$$

The function F increases monotonically with M and becomes nearly linear for M greater than eight. Probstein⁵ has recently suggested a value for the proportionality constant between λ and $1/\rho$, the use

of which in the above equation for λ results in

$$\lambda p_t = 3.97 \times 10^{-11} \frac{p_t}{p} R T F(M),$$

a function of Mach number and total temperature.

Muckenfuss also concludes that the simple $1/\rho$ dependence of λ is inaccurate for real gases, and that λ should generally vary with the viscosity. However, in the absence of a more generally agreed upon form for the variation of the mean free path of a stationary gas, the inverse dependence upon density was chosen for use in this report. Figure 5 is a plot of the foregoing equation for λp_t versus Mach number for various total temperatures.

A RELATION BETWEEN KNUDSEN, MACH, AND REYNOLDS NUMBERS

We now have both the Reynolds and Knudsen numbers (based on unit length and unit total pressure) given as functions of Mach number and total temperature. This suggests the possibility of eliminating T_t and attempting to find Kn as a function of M and Re only. The form of this function may be approximated⁷ by letting viscosity behave as predicted by rigid sphere kinetic theory ($\mu \sim \rho \lambda a$, in which λ refers to static mean free path) and assuming F to be proportional to Mach number. Then it follows immediately that

$$Kn \sim \frac{M^2}{Re} .$$

In fact, the data used for the graphs in this report yield a value of $Kn Re / M^2$ which varies from about 0.9 to 3.9 for Mach numbers from 0.5 to 30 and total temperatures from 600° to 5000°R. Considering the crudeness of the approximate relation, this spread (which results primarily from the discrepancy in viscosity laws) is relatively small.

Contrails

So the possibility arises that we may find an empirical relation of the form

$$\frac{KnRe}{M^2} = \sum_{i=0}^I \sum_{j=0}^{J-i} C_{ij} \text{Ln}^i Re \text{Ln}^j M, \quad J \geq I.$$

The logarithms of M and Re are used because of the large variation of M and Re compared to the corresponding variation of $KnRe/M^2$.

A bivariate least squares fit to all the calculated data points (M, Re, Kn), for which the static temperature was 20°R or greater, was used to obtain the C_{ij} for various values of I and J. Of the various functions that resulted from different selections of I and J, two are presented here. The simpler (I = 1, J = 2) gives a root mean square error in Kn of 8.5% and a maximum error of 28.7%. The more complex function (I = 2, J = 4) gives a root mean square error in Kn of 4.6% with a 13.3% maximum error. The functions are

$$Kn = \frac{M^2}{Re} (-1.09 - 1.81 \text{Ln} M + 0.301 \text{Ln} Re + 0.974 \text{Ln}^2 M + 0.107 \text{Ln} M \text{Ln} Re),$$

and

$$Kn = \frac{M^2}{Re} (4.544 - 1.042 \text{Ln} M - 0.9386 \text{Ln} Re - 0.6130 \text{Ln}^2 M + 0.05205 \text{Ln} M \text{Ln} Re + 0.06869 \text{Ln}^2 Re + 0.1413 \text{Ln}^3 M + 0.08289 \text{Ln}^2 M \text{Ln} Re - 0.006913 \text{Ln} M \text{Ln}^2 Re + 0.03366 \text{Ln}^4 M + 0.01220 \text{Ln}^3 M \text{Ln} Re + 0.006696 \text{Ln}^2 M \text{Ln}^2 Re).$$

These functions were computed for, and the above errors refer to, the range $0.5 \leq M \leq 30$ and $200^\circ R \leq T_t \leq 5000^\circ R$, with the additional restriction $T \geq 20^\circ R$. This range is illustrated in Figure 6.

COMMENT ON THE UNCERTAINTY OF THE GRAPHS

The data herein presented were calculated to four significant figures. The range of validity of the graphs is imposed by the assumptions of the analysis, for example, that the air is condensation free and gamma is independent of pressure. Within this range, the limits on the accuracy of the graphs result from their plotting and reading, and from the uncertainty of the inputs to the calculations, for example, the low temperature viscosity. The latter uncertainty can be assessed only as new information becomes available. We have, however, estimated the uncertainty due to plotting and reading by employing an independent observer to read values from the finished graphs and compare these values with the computed ones. This test resulted in a root mean square error for Figures 1 and 2 of 0.2%, with 95% of the readings less than 0.4% in error, and a root mean square error for Figures 3, 4 and 5 of 1.1%, with 95% of the readings less than 2.0% in error. This test did not include interpolation between curves.

REFERENCES

1. Ames Research Staff, "Equations, Tables, and Charts for Compressible Flow." NACA Report 1135, 1953.
2. Daum, F. L., "The Condensation of Air in a Hypersonic Wind Tunnel." AIAA Journal, Volume 1, Number 5, pp 1043-1046, May 1963.
3. Bromley and Wilke, "Viscosity at Low Temperatures." University of California TR HE-150-157.
4. Gregorek, G. M. and Lee, J. D., "Design Performance and Operational Characteristics of the ARL Twenty-Inch Hypersonic Wind Tunnel." Aeronautical Research Laboratories Report ARL 62-392, August 1962.
5. Probstein, R. F., "Heat Transfer in Rarefied Gas Flow." Research in Heat Transfer, pp 33-60, Pergamon Press, London, 1963.
6. Muckenfuss, C., "Mean-Free-Path Concept in Gas Dynamics." Physics of Fluids, Volume 5, Number 3, pp 165-168, February 1962.
7. Hayes, W. D. and Probstein, R. F., Hypersonic Flow Theory, Academic Press, New York, 1959.

Contrails

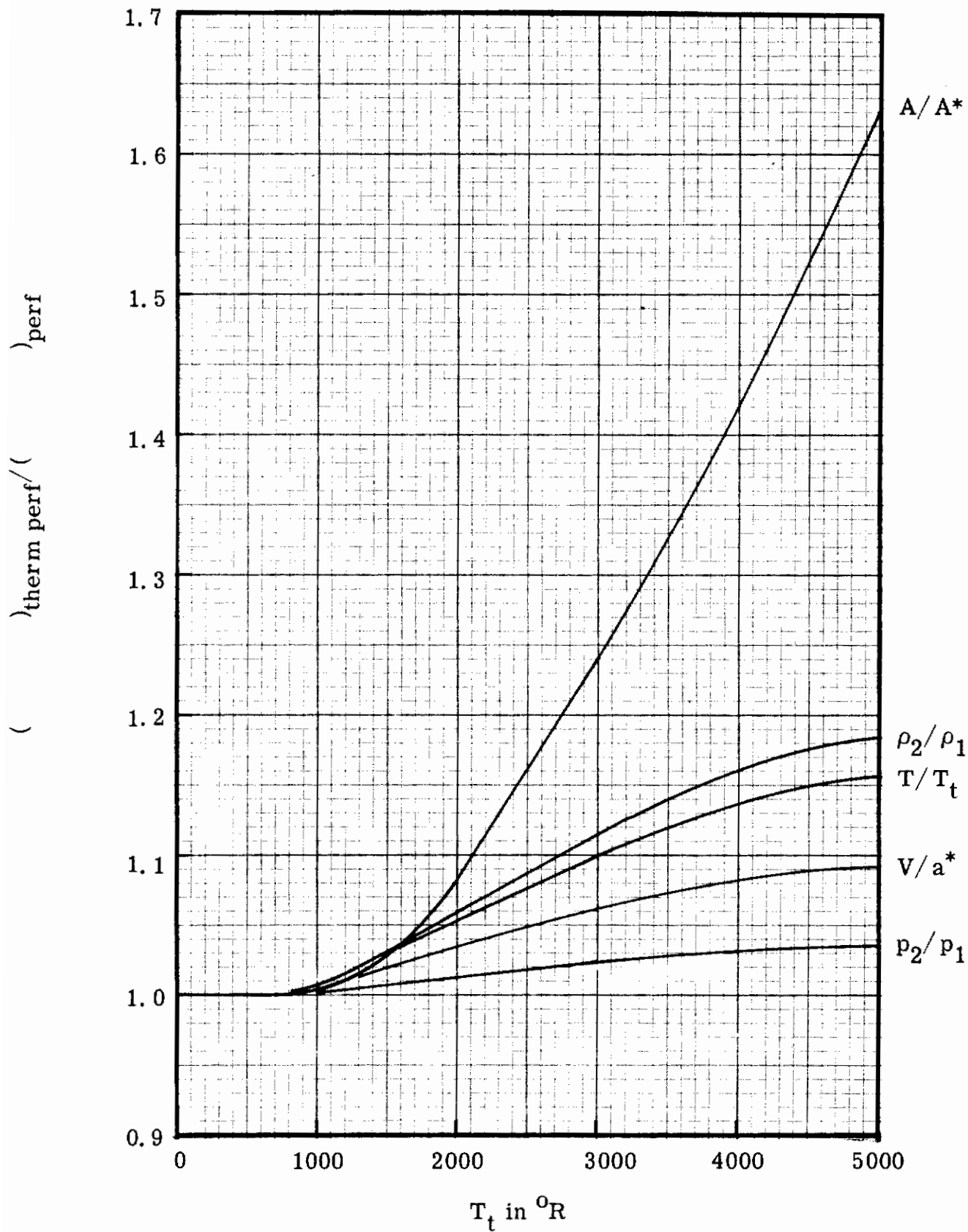


Figure 1a: Effect of caloric imperfections on one-dimensional flow properties (for Mach numbers greater than seven) plotted versus total temperature.

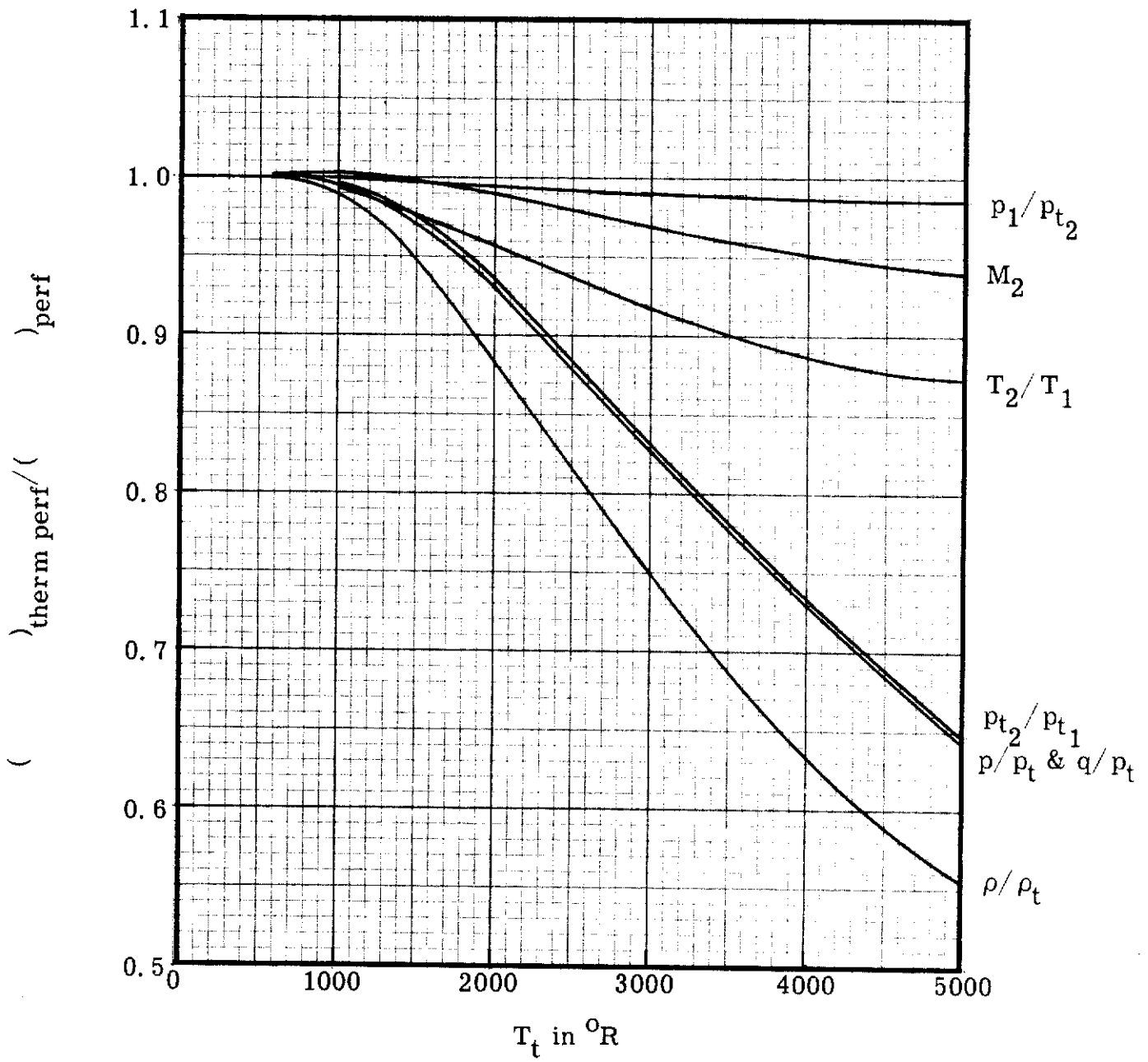


Figure 1b: Effect of caloric imperfections on one-dimensional flow properties (for Mach numbers greater than seven) plotted versus total temperature.

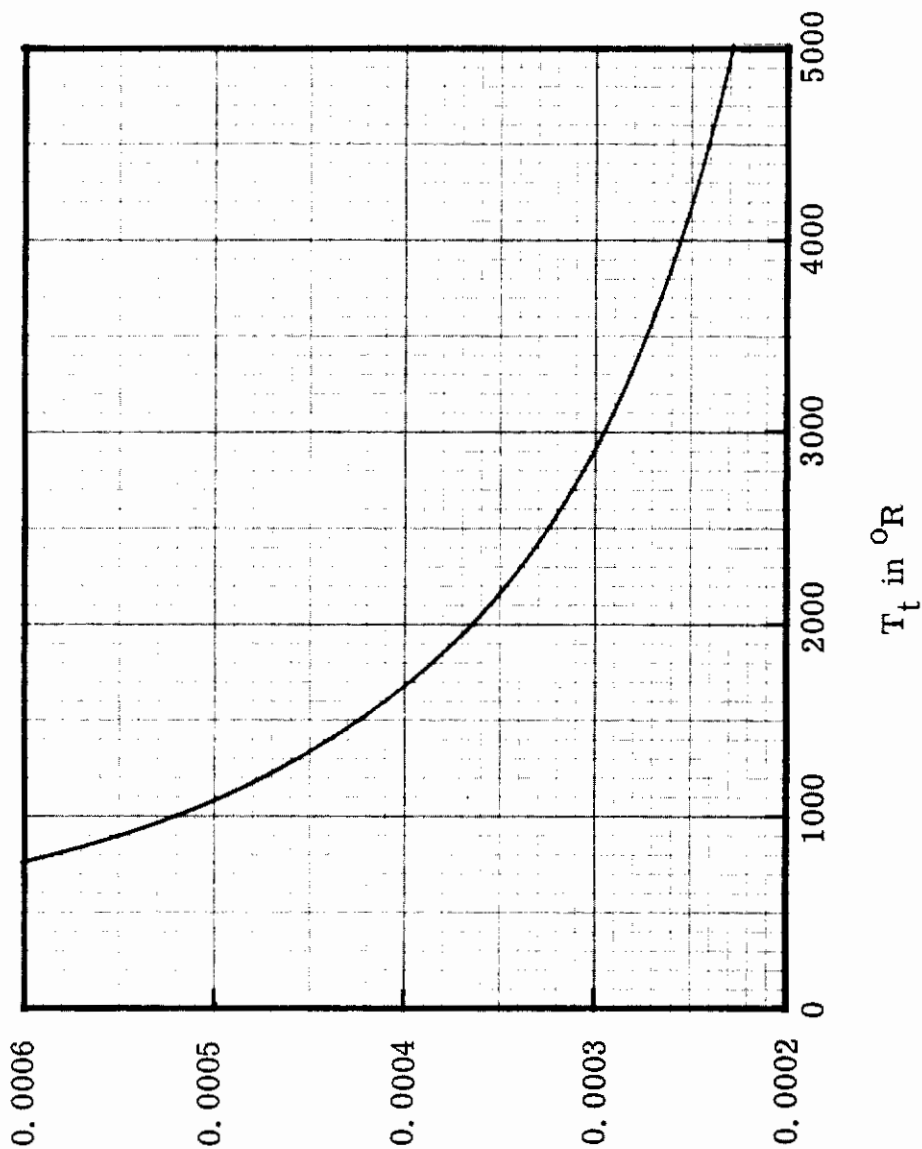


Figure 2: Mass flow rate of air per unit throat area, per unit total pressure versus total temperature.

$$\frac{m}{A p_t} = \frac{\rho^* V^*}{p_t} \text{ in } \frac{\text{Slugs}}{\text{Sec Lbl}}$$

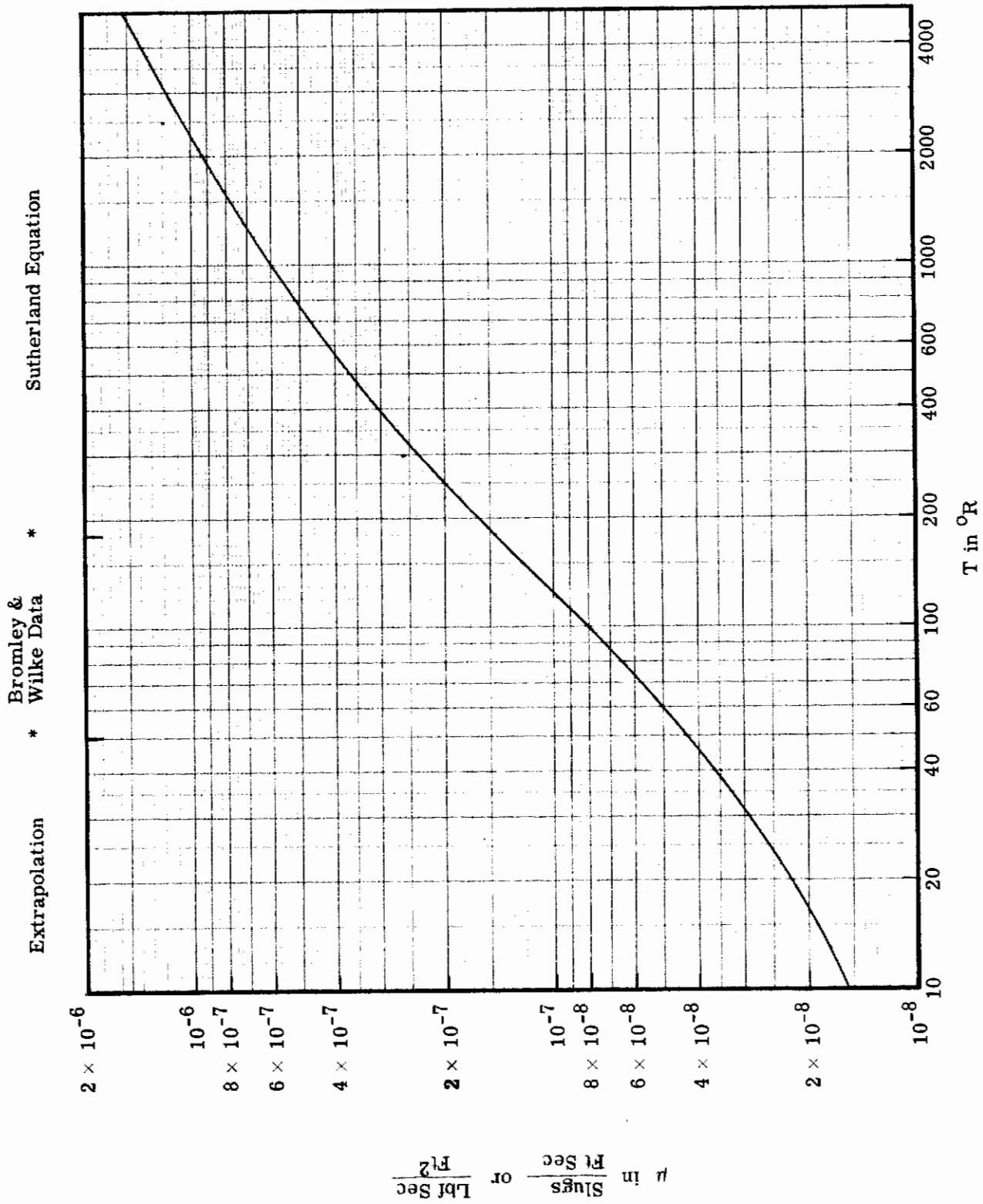


Figure 3: Viscosity of air versus temperature.

Contrails

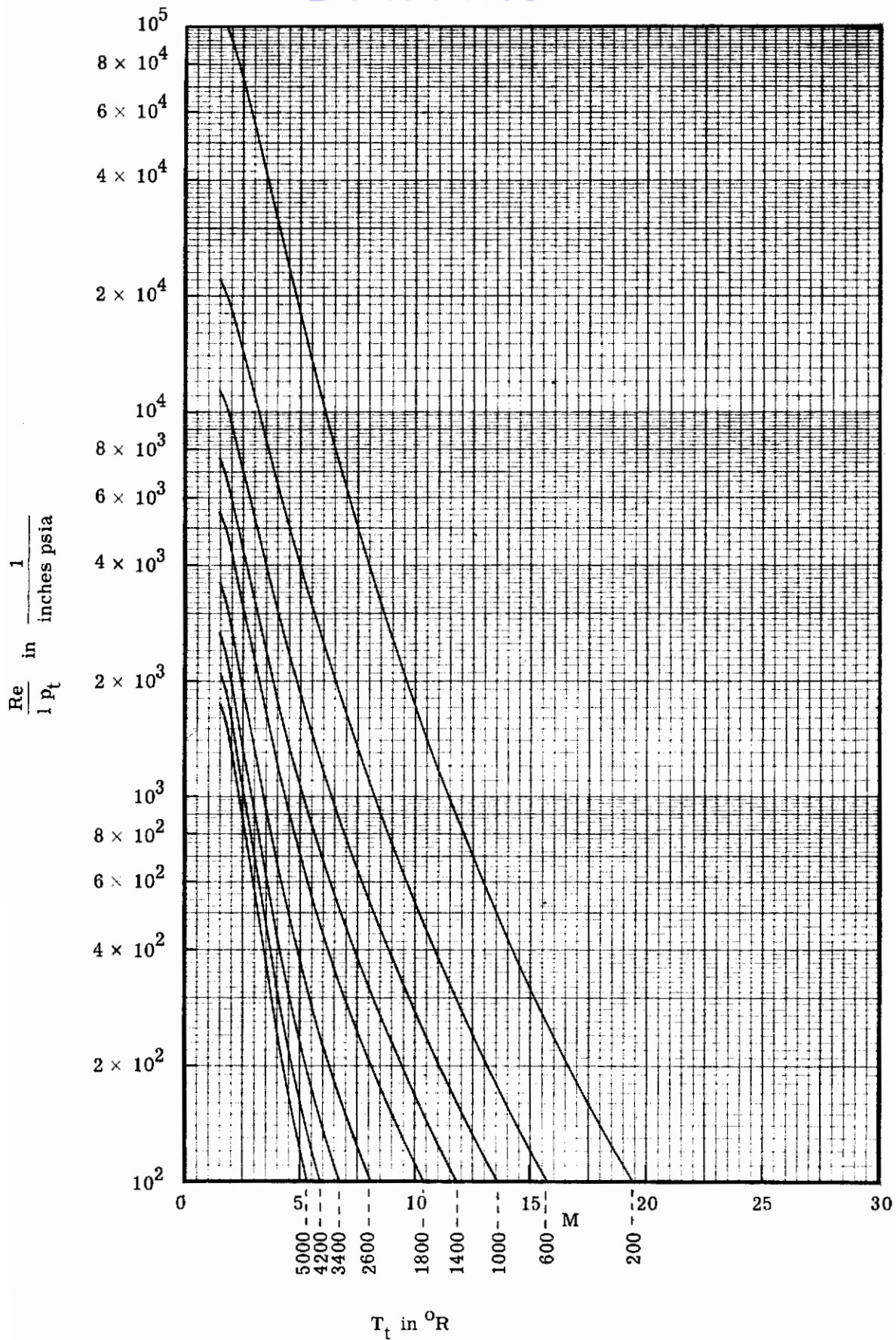


Figure 4a: Reynolds number per unit length, per unit total pressure versus Mach number for various total temperatures.

Contrails

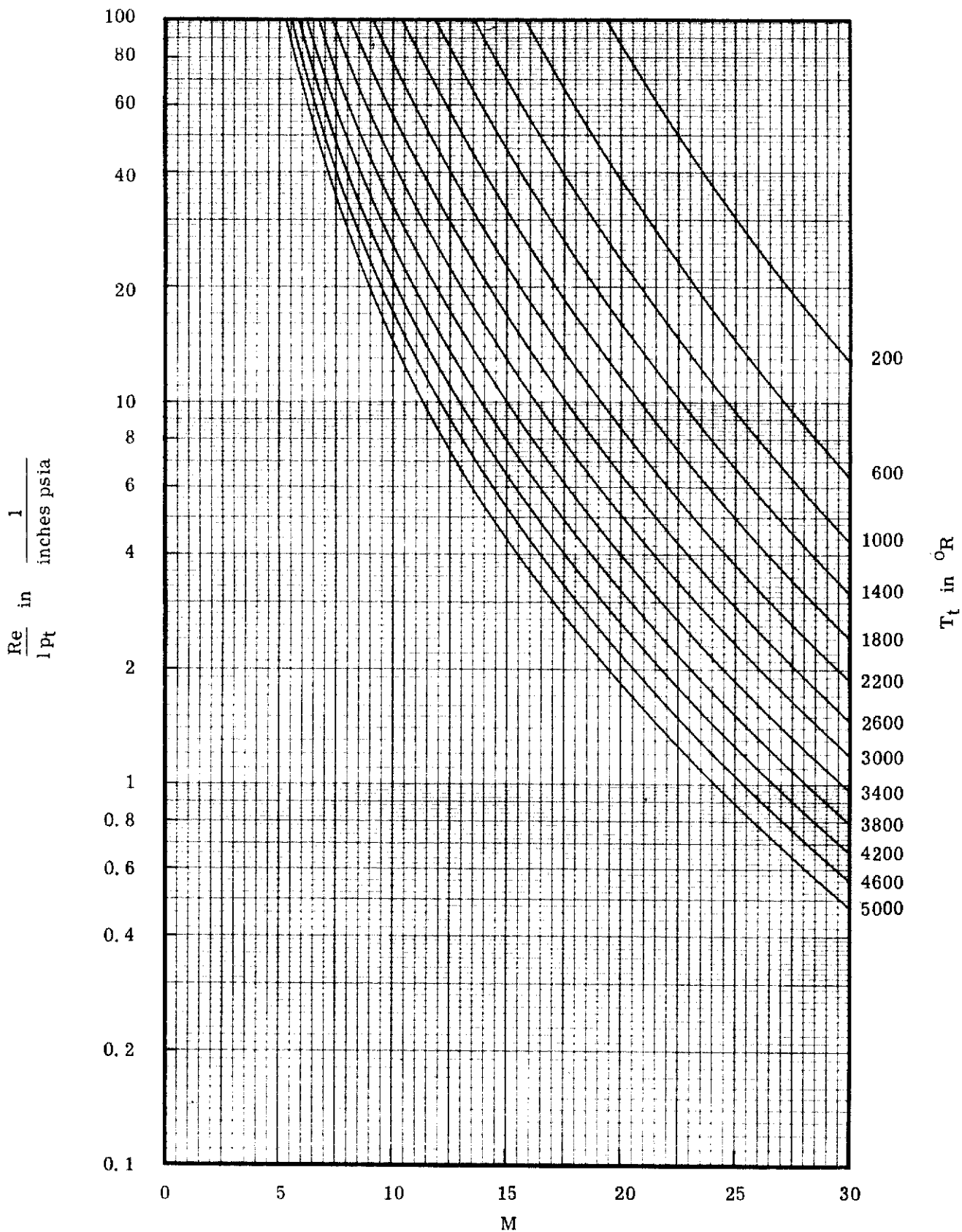


Figure 4b: Reynolds number per unit length, per unit total pressure versus Mach number for various total temperatures.

T_t in $^{\circ}R$

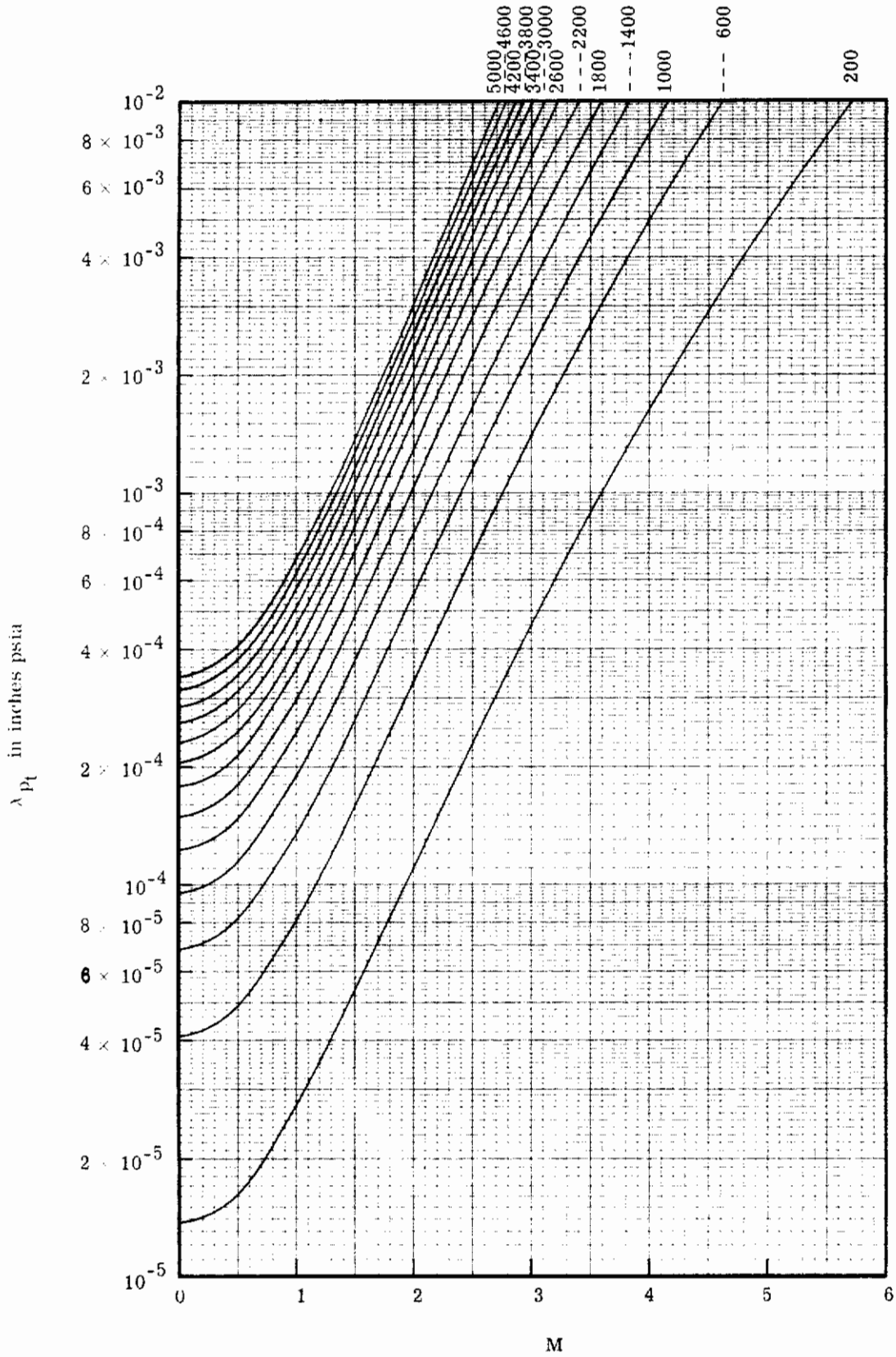


Figure 5a: Mean free path times total pressure versus Mach number for various total temperatures.

T_t in $^{\circ}R$

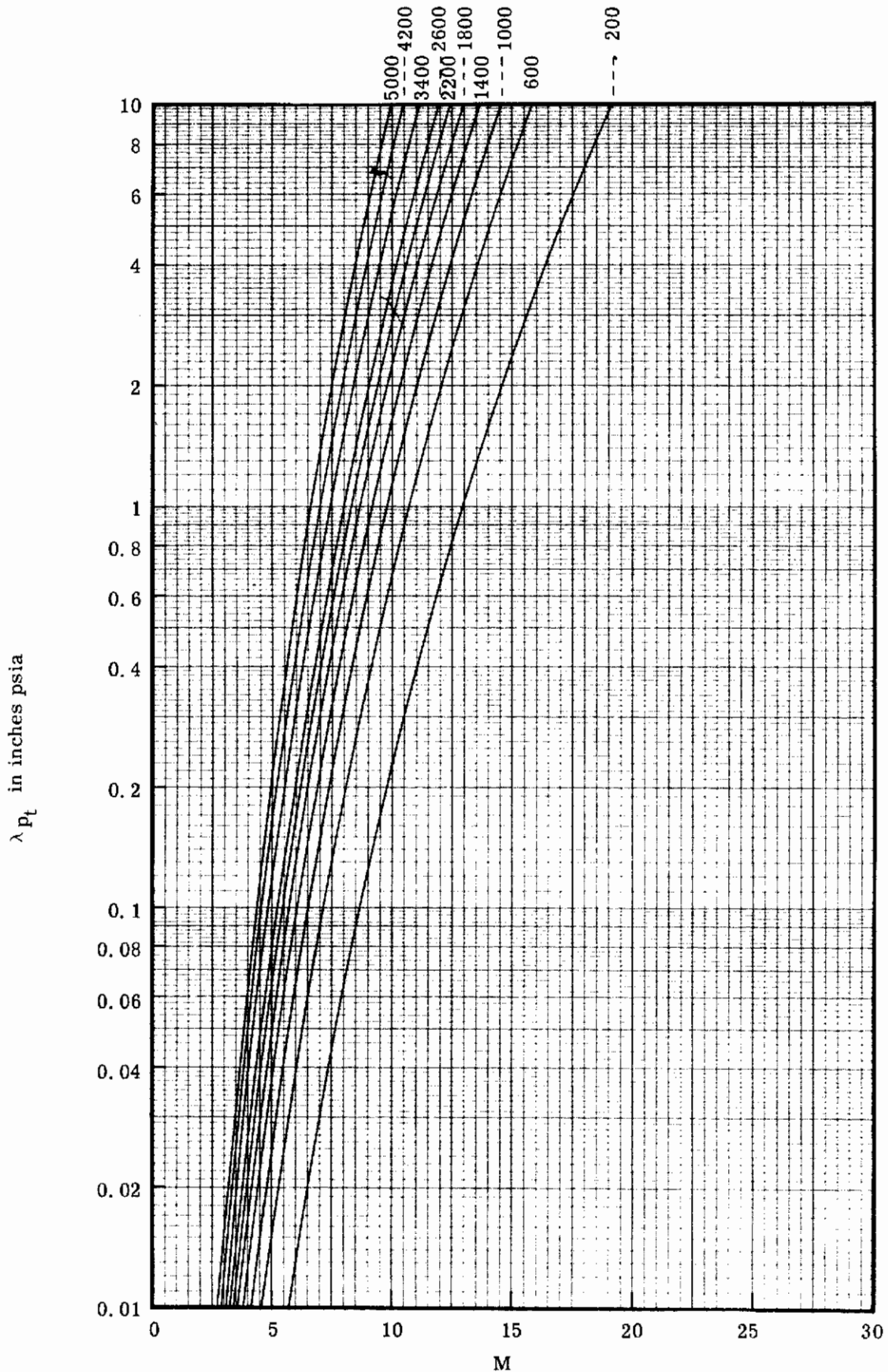


Figure 5b: Mean free path times total pressure versus Mach number for various total temperatures.

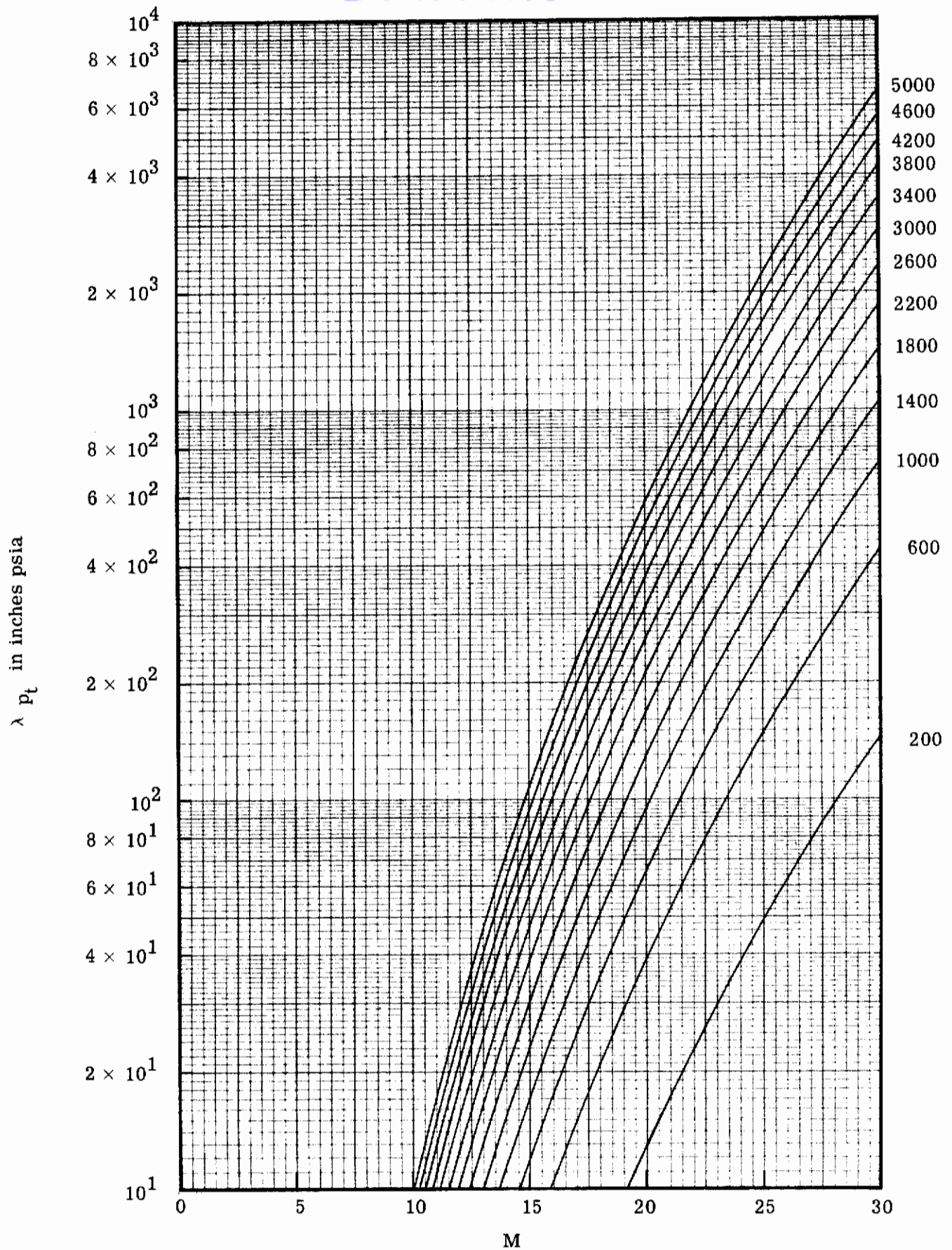


Figure 5c: Mean free path times total pressure versus Mach number for various total temperatures.

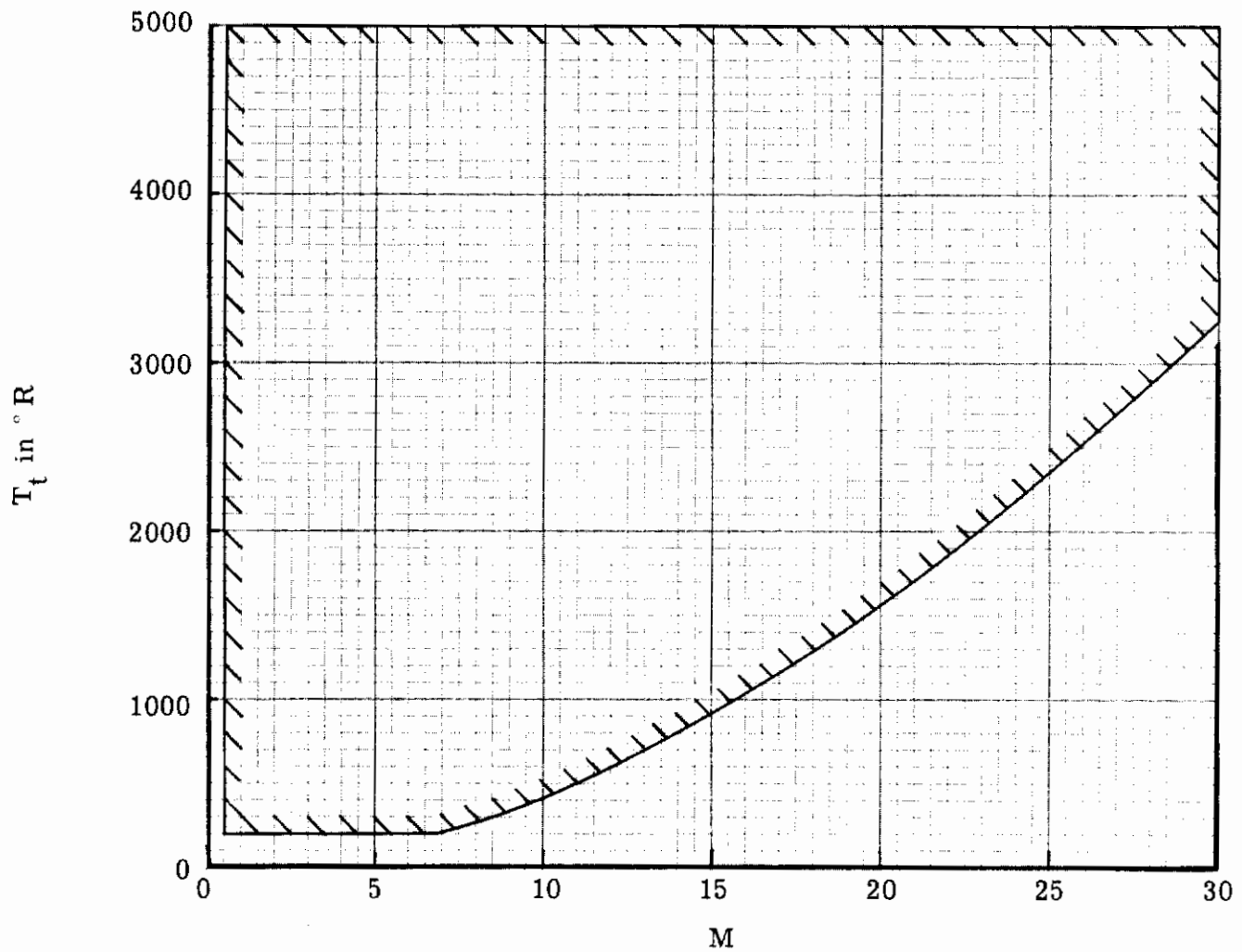


Figure 6: Values of total temperature and Mach number satisfying the inequalities: $0.5 \leq M \leq 30$, $200^\circ \text{R} \leq T_t \leq 5000^\circ \text{R}$, $T \geq 20^\circ \text{R}$.